Spatiotemporal responses in crop water footprint and benchmark under different irrigation techniques to climate change scenarios in China

Zhiwei Yue[1, 3,*], Xiangxiang Ji[1, 3,*], La Zhuo[2, 3, 4, 5], Wei Wang[4,5], Zhibin Li[4,5], Pute Wu[2, 3, 4, 5]

[1]College of Water Resources and Architectural Engineering, Northwest A&F University, Yangling 712100, China
[2]Institute of Soil and Water Conservation, Northwest A&F University, Yangling 712100, China
[3]Institute of Water-saving Agriculture in Arid Regions of China, Northwest A&F University, Yangling 712100, China
[4]Institute of Soil and Water Conservation, Chinese Academy of Sciences and Ministry of Water Resources, Yangling 712100, China
[5] University of Chinese Academy of Sciences, Beijing 100049, China.

*These authors contributed equally to this work.

Correspondence to: La Zhuo (zhuola@nwafu.edu.cn; lzhuo@ms.iswc.ac.cn) and Pute Wu (gjzwpt@hotmail.com)

Abstract. Adaptation to future climate change with limited water resources is a major global challenge to sustainable and sufficient crop production. However, the large-scale responses of crop water footprint and its associated benchmarks under various irrigation techniques to future climate change scenarios remain unclear. The present study quantified the responses of maize and wheat water footprint per unit yield (WFP, $m^3 \, t^{-1}$) and corresponding WFP benchmarks under two representative concentration pathways (RCPs) in the 2030s, 2050s, and 2080s at a 5-arc minute grid level in the case for China. The differences among rain-fed and furrow-, micro-, and sprinkler-irrigated wheat and maize were identified. Compared with the baseline year (2013), maize WFP will increase under both RCP2.6 and RCP8.5, by 17 % and 13 %, respectively, until the 2080s. Wheat WFP will increase under RCP2.6 (by 12 % until the 2080s), while decrease by 12 % under RCP8.5 until the 2080s. WFP will increase the most for rain-fed crops. Relative to rain-fed crops, micro irrigation and sprinkler irrigation result in the smallest increases in WFP for maize and wheat, respectively. These water-saving managements will more effectively mitigate the negative impact of climate change. Furthermore, the spatial distributions of WFP benchmarks will not change as dramatically as those of WFP. The present study demonstrated that the visible different responses to climate change in terms of crop water consumption, water use efficiency, and WFP benchmarks under different irrigation techniques must be addressed and monitored. It also lays the foundation for future investigations into the influences of irrigation methods, RCPs, and crop types on WFP and its benchmarks in response to climate change in all agricultural regions worldwide.

1 Introduction

The progressive decline in water resource availability is a major impediment to global food production security (Pastor et al., 2019; Trnka et al., 2019; Konapala et al., 2020). Food crops are the main source of human nutrition (Myers et al., 2017; Lobell and Gourdji, 2012). Humans depend on food crops for ~47 % of their daily protein intake (FAO, 2021). As a result of human activity, however, the climate system is changing and global warming is a significant characteristic of this process (IPCC, 2021). Global mean temperatures have increased with each successive decade since 1850 (Kappelle, 2020). Climate change affects water consumption and crop yield by altering precipitation, temperature, carbon dioxide (CO_2) concentration, and other factors during crop growth (Hatfield and Dold, 2019). Crop adaptation to future climate change with limited water resources has become a major challenge in sustainable crop production and supply worldwide.

The water footprint per unit crop (WFP, m^3 t^{-1}) (Hoekstra, 2003) is the amount of water consumed by the crop per unit yield during crop growth within a certain region. It includes blue WFP (surface and groundwater), green WFP (precipitation that will not become runoff), and grey WFP (freshwater that needed to assimilate pollutants from human activities) (Hoekstra et al., 2011). Blue and green WFP are collectively known as consumptive WFP. Grey WFP is also called degradative WFP (Hoekstra, 2013). Unlike traditional crop water productivity and other agricultural water metrics, WFP covers water consumption, sources, and spatiotemporal dimensions during the crop growth period. In this way, water consumption intensity and efficiency for irrigated and rain-fed planting modes may be compared. WFP is an effective indicator of the sustainability of regional water use and optimal water resource allocation (Xu et al., 2019; Mali et al., 2021). The present study focuses exclusively on consumptive WFP which depends on crop yield and the intensity of water consumption per unit planted area.

There are several studies conducted on the responses of WFP to future climate change. Nevertheless, no consensus has been reached. Certain scholars believe that future climate change will weaken food crop production security. Ahmadi et al. (2021) reported that maize WFP in the Qazvin Plain of India will increase by 42 % and 147 % under representative concentration pathways (RCP) 4.5 and RCP8.5, respectively, by 2061–2080. Zheng et al. (2020) found that rice yield in Henan and Jiangsu (China) will decrease while WFP will increase under four RCPs at various stages of the 21st century. Other scholars believe that crop yield may actually benefit from future increases in precipitation and atmospheric CO_2 concentration. Jans et al. (2021) considered the combined effects of changes in climatic factors such as temperature and precipitation as well as rising atmospheric CO_2 concentration and predicted that between 2011 and 2099, global cotton yield will increase by > 50 % and WFP will decrease by 30 % under RCP8.5. Arunrat et al. (2020) found that in the present century, the yield of individual and large-scale rice farms in Thailand will increase by 1–30 % and 2–31 %, respectively, while WFP will decrease by 10–43 % and 1–67 %, respectively, under RCP4.5. Significant spatiotemporal differences in WFP under various irrigation techniques have been confirmed at the site (Chukalla et al., 2015) and regional (Wang et al., 2019) scales. However, current large-scale studies on the responses of WFP to environmental change are usually based on simulations assuming adequate furrow irrigation. These studies exclude comparisons between various irrigation techniques and the differences in their influences on crop WFPs.

Although Dai et al. (2020) optimised maize and wheat cropping patterns under RCP4.5 and RCP8.5 with consideration of various irrigation modes in the case for the Huaihe River Basin of China by 2050, they only considered blue water.

Magnitudes and constitution of crop WFP varies widely among regions and areas (Mekonnen and Hoekstra, 2011). To
65   encourage water users to reduce WFP to a reasonable level, Hoekstra (2013, 2014) recommended establishing WFP benchmarks for different products as they facilitate prudent water allocation and fair water resource sharing among sectors and users (Hoekstra, 2013). On the large-scale, specific WFP benchmarks can be set for crops grown on different farms within the same region (Mekonnen and Hoekstra, 2014). A previous study demonstrated the sensitivity of WFP benchmarks to climate zones (Zhuo et al., 2016a). WFP benchmarks significantly differ among irrigation techniques, especially in arid zones (Wang
70   et al., 2019). However, little is known about the responses of WFP benchmarks under different irrigation techniques to future climate change.

To probe into the influence of future climate change on large-scale WFP and benchmarks under diverse irrigation techniques, the research cases used here were maize and wheat grown in mainland China. We used the outputs of six global climate models (GCMs) (Table 1), including three models each for relatively wet and dry climate outputs, in Coupled Model
75   Intercomparison Project Phase 5 (CMIP5). We then used the AquaCrop model to simulate the spatiotemporal responses of blue and green WFP and corresponding WFP benchmarks for wheat and maize in the 2030s (2020–2049), 2050s (2040–2069), and 2080s (2070–2099) under RCP2.6 and RCP8.5 at a 5-arc minute grid resolution. We distinguished between rain-fed and irrigated planting modes and among furrow, micro, and sprinkler irrigation.

As of 2019, China was the world's second largest maize and largest wheat producer, accounting for 23 % and 17 % of
80   total global production, respectively (FAO, 2021). China's cereal production has helped stabilise global food production and supply. In 2019, the planted areas of maize and wheat in China were 41 million ha and 24 million ha, respectively, and accounted for 25 % and 14 % of the national total croplands, respectively (NBSC, 2021). Cereal production consumes substantial volumes of water in China and these quantities change over time. Zhuo et al. (2019) reported that maize water consumption increased by 49 % between 2000 and 2013 as planted areas and feed demand increased. By contrast, Wang et al.
85   (2019) reported that wheat planted and irrigated areas decreased and water consumption slightly declined (4.4 %) from 2000 to 2014. Other studies reported that maize and wheat consume relatively more water in the North than the South of China (Tian et al., 2019; Wang et al., 2019). Therefore, the water consumption rates of these staple crops under future climate change scenarios should be closely monitored to ensure water supply and food crop production security in China and worldwide. Compared with existing researches, the innovations of our research are embodied in two points. The present study firstly
90   clarifies large-scale spatiotemporal responses of WFP to future climate change scenarios under different irrigation techniques. It is also the first to explore large-scale changes in WFP benchmarks under future climate change scenarios.

Table 1. Inventory of global climate models (GCMs) used in the current study.

GCM	Institute	Reference	Type

CCCMA-CanESM2	Canadian Centre for Climate Modelling and Analysis	Arora et al. (2011); von Salzen et al. (2013)	Wet
CESM1-CAM5	National Science Foundation, Department of Energy, National Center for Atmospheric Research	Hurrell et al. (2013)	
GFDL-CM3	NOAA Geophysical Fluid Dynamics Laboratory	Delworth et al. (2006); Donner et al. (2011)	
FIO-ESM	The First Institute of Oceanography, State Oceanic Administration, China	Qiao et al. (2013)	Dry
GISS-E2R	NASA Goddard Institute for Space Studies USA	Schmidt et al. (2006); Schmidt et al. (2014)	
IPSL-CM5A-MR	Institute Pierre Simon Laplace	Dufresne et al. (2013)	

2 Method and data

2.1 Determining the baseline year

Annual reference evapotranspiration (ET_0, mm) and precipitation (PR, mm) in China were calculated (Harris et al., 2014). Thence, the aridity index (AI) was calculated and climate change trends from 2000 to 2014 were analysed. The year 2013 was designated the baseline as its drought level was nearest the 15-year national average. The AI was calculated according to the method of Middleton and Thomas (1997):

$$AI = \frac{PR}{ET_0}, \tag{1}$$

2.2 Water footprint per unit crop calculation

WFP (m^3 t^{-1}) comprises blue WFP (WFP$_b$, m^3 t^{-1}) and green WFP (WFP$_g$, m^3 t^{-1}):

$$WFP = WFP_b + WFP_g, \tag{2}$$

where WFP_b and WFP_g were calculated as the quotient of the blue (CWU_b, m^3 ha^{-1}) and green (CWU_g, m^3 ha^{-1}) components of crop water use (CWU, m^3 ha^{-1}) and crop yield (Y, t ha^{-1}), respectively. CWU_b and CWU_g were equivalent to the cumulation of daily evapotranspiration (ET, mm d^{-1}) throughout the whole crop growth period (Hoekstra et al., 2011):

$$WFP_b = \frac{CWU_b}{Y} = \frac{10 \times \sum_{d=1}^{lgp} ET_b}{Y}, \tag{3}$$

$$WFP_g = \frac{CWU_g}{Y} = \frac{10 \times \sum_{d=1}^{lgp} ET_g}{Y}, \tag{4}$$

where ET_b and ET_g (mm) refer to the blue and green water evapotranspiration, respectively, and lgp refers to the number of days of the crop growth period. The coefficient 10 is a unit conversion factor, transforming the water depth of ET (mm) into the water amount per unit land area of CWU (m^3 ha^{-1}).

The ET and Y per grid for each crop were simulated by AquaCrop model based on the dynamic daily soil water balance (Mekonnen and Hoekstra, 2010):

$$S_{[t]}=S_{[t-1]}+PR_{[t]}+IRR_{[t]}+CR_{[t]}-ET_{[t]}-RO_{[t]}-DP_{[t]} \,, \tag{5}$$

where $S_{[t]}$ and $S_{[t-1]}$ (mm) refer to the water content in soil when the day t ends and begins, respectively, $PR_{[t]}$ (mm) is the amount of precipitation on day t, $IRR_{[t]}$ (mm) is the amount of water used for irrigation, $CR_{[t]}$ (mm) is the capillary rise to the crop root zone from the shallow groundwater, $RO_{[t]}$ (mm) is the water lost by surface runoff due to precipitation, and $DP_{[t]}$ (mm) is the water lost by deep percolation caused by excessive precipitation or irrigation. It was assumed that $CR_{[t]} = 0$ as the

115 ground water depth was $\gg 1$ m (Allen et al., 1998). $RO_{[t]}$ was calculated using the Soil Conservation Service curve-number (CN) equation (USDA, 1964; Rallison, 1980):

$$RO_{[t]}=\frac{(PR_{[t]}-I_a)^2}{PR_{[t]}+S-I_a} \,, \tag{6}$$

$$S=254(\frac{100}{CN}-1) \,, \tag{7}$$

where S (mm) is the potential maximum water storage, I_a (mm) is the initial amount of water loss before the runoff formation.

   By tracking the daily flow of water in and out of the crop root zone, we separated the daily blue and green soil water balances (Zhuo et al., 2016b):

$$S_{b[t]}=S_{b[t-1]}+\left(PR_{[t]}+IRR_{[t]}-RO_{[t]}\right)\times\frac{IRR_{[t]}}{PR_{[t]}+IRR_{[t]}}-\left(DP_{[t]}+ET_{[t]}\right)\times\frac{S_{b[t-1]}}{S_{[t-1]}} \,, \tag{8}$$

$$S_{g[t]}=S_{g[t-1]}+\left(PR_{[t]}+IRR_{[t]}-RO_{[t]}\right)\times\frac{PR_{[t]}}{PR_{[t]}+IRR_{[t]}}-\left(DP_{[t]}+ET_{[t]}\right)\times\frac{S_{g[t-1]}}{S_{[t-1]}} \,, \tag{9}$$

120 where $S_{b[t]}$ and $S_{b[t-1]}$ (mm) are the blue water content in soil when the day t ends and begins, respectively, and $S_{g[t]}$ and $S_{g[t-1]}$ (mm) are the green water content in soil when the day t ends and begins, respectively. It is assumed that the initial soil water content before the crop growth period is green water.

   In AquaCrop, the daily transpiration ($Tr_{[t]}$, mm) calculates the daily shoot biomass production (B, kg) using the normalised crop biomass water productivity (WP^*, kg m^{-2}) (Raes et al., 2017):

$$B=WP^*\times\sum\frac{Tr_{[t]}}{ET_{0[t]}} \,, \tag{10}$$

125 where WP^* is normalised to consider CO_2 concentration, reference evapotranspiration (ET_0), and crop classes (C3 or C4) so that it is applicable to various locations and seasons. Water productivity remains constant for specific crops. Y as the harvestable portion of final B is calculated by multiplying B with the adjusted reference Harvest Index (HI_0, %):

$$Y=f_{HI}\times HI_0\times B \,, \tag{11}$$

where f_{HI} is a correction factor for HI_0. It considers the water and temperature stresses during the crop growth period. The simulated Y per grid for each crop in 2013 was validated via scaling model simulation outputs to accord with the crop yield

130 statistics data at the provincial level (NBSC, 2021), following Zhuo et al. (2016c) and Mialyk et al. (2021).

2.3 Benchmarking consumptive WFP in crop production

   Based on the work of Mekonnen and Hoekstra (2014), we ranked grid-level WFP for each crop in ascending order of size against the corresponding accumulative percentages of the total crop production. The annual WFP of 20 % or 25 % of the

producers with the highest water productivity in China was set as the annual WFP benchmark. The climate zones should be

135 divided when WFP benchmarks were established (Zhuo et al., 2016a). To this end, the aridity index (AI) partitioned China

into arid (< 0.5) and humid (> 0.5) zones based on the annual ET_0 and PR from 2000 to 2014 at a 30-arc minute grid resolution

(Harris et al., 2014) (Fig. 1).

Figure 1. Regions and climate zones of mainland China.

140

2.4 Data sources

Monthly climate data such as maximum (Tx), minimum air temperature (Tn), precipitation (PR) and reference

evapotranspiration (ET_0) from 2000 to 2014 at a resolution of 30-arc minute were derived from the CRU-TS 3.24 dataset

(Harris et al., 2014; CEDA, 2018). The mean annual atmospheric CO_2 concentration (ppm) from 2000 to 2014 was obtained

145 from the Mauna Loa Observatory, Hawaii, USA (NOAA, 2018). The downscaled outputs of six GCMs at a 5-arc minute grid

resolution in the 2030s, 2050s, and 2080s were obtained from the Climate Change, Agriculture and Food Security (CCAFS)

database (Navarro-Racines et al., 2020; CCAFS, 2015). As the CCAFS database has not ET_0 data, we calculated ET_0 for each

climate scenario using temperature inputs and the Penman-Monteith method (Allen et al., 1998). The projected CO_2

concentrations under RCP2.6 and RCP8.5 were obtained from van Vuuren et al. (2007) and Riahi et al. (2007), respectively.

150 The selected maximum root depth (Zx) and Harvest Index (HI) in AquaCrop were derived from Allan et al. (1998). And the

other parameters used in AquaCrop were derived from Raes et al. (2017). Soil texture data and soil water capacity data at a 5-

arc minute grid resolution were acquired from the ISRIC Soil and Terrain database (Dijkshoorn et al., 2008) and ISRIC-WISE

dataset (Batjes, 2012), respectively. The planted areas for each irrigated or rain-fed crop at a 5-arc minute grid resolution were

acquired from the MIRCA2000 dataset (Portmann et al., 2010). We divided these planted areas into different parts subjected
155 to various irrigation techniques using statistical yearbook data (NBSC, 2021). Provincial-level crop yield statistics data were
procured from the National Bureau of Statistics of China (NBSC, 2021).

3 Results

3.1 Future climate change trends in maize and wheat planted areas

In the baseline year 2013, the average annual reference evapotranspiration (ET_0) and precipitation (PR) in the planted
160 areas of two crops were 941 mm and 727 mm, respectively. Compared with the baseline level of 2013, the average annual ET_0
and PR in the planted areas of two crops will both increase under two RCPs. The increase in ET_0 exceeds that of PR. ET_0 will
increase by 17 % and 29 % under RCP2.6 and RCP8.5, respectively, until the 2080s. However, PR will increase by 8 % and
14 %, respectively. The increases under RCP8.5 (18–29 % and 3–14 % for ET_0 and PR, respectively) are much higher than
those under RCP2.6 (16–17 % and 4–8 % for ET_0 and PR, respectively). Climate change will be relatively more intense under
165 RCP8.5. The increases in ET_0 are concentrated from April to August (14–39 mm). The increases in PR increases are
concentrated between June and August (8–20 mm and 12–28 mm, respectively). However, PR will decline in May, July,
November, and December while PR will decline more in May ($\leq$ 9 mm until the 2030s) (Fig. 2a, b). Water and heat resources
were unevenly distributed in the planted areas of the two crops in 2013. ET_0 was relatively higher in East Coast and North
China. PR distribution was comparatively higher in the South and lower in the North (Fig. S4). Compared with 2013, ET_0 and
170 PR for the most heavily planted areas will increase under both scenarios until the 2080s. The areas with relatively greater
increase in ET_0 are distributed mainly in Southwest and Northeast (Fig. 2c, e). PR increases relatively faster in Northwest and
Jing-Jin (Fig. 2d, f). ET_0 decreases mainly in Xinjiang and Inner Mongolia (Fig. 2c, e). PR decreases mainly in Xinjiang, Tibet,
Northeast, and South Coast (Fig. 2d, f). However, the areas wherein ET_0 falls are 86–94 % smaller than those wherein PR
declines.
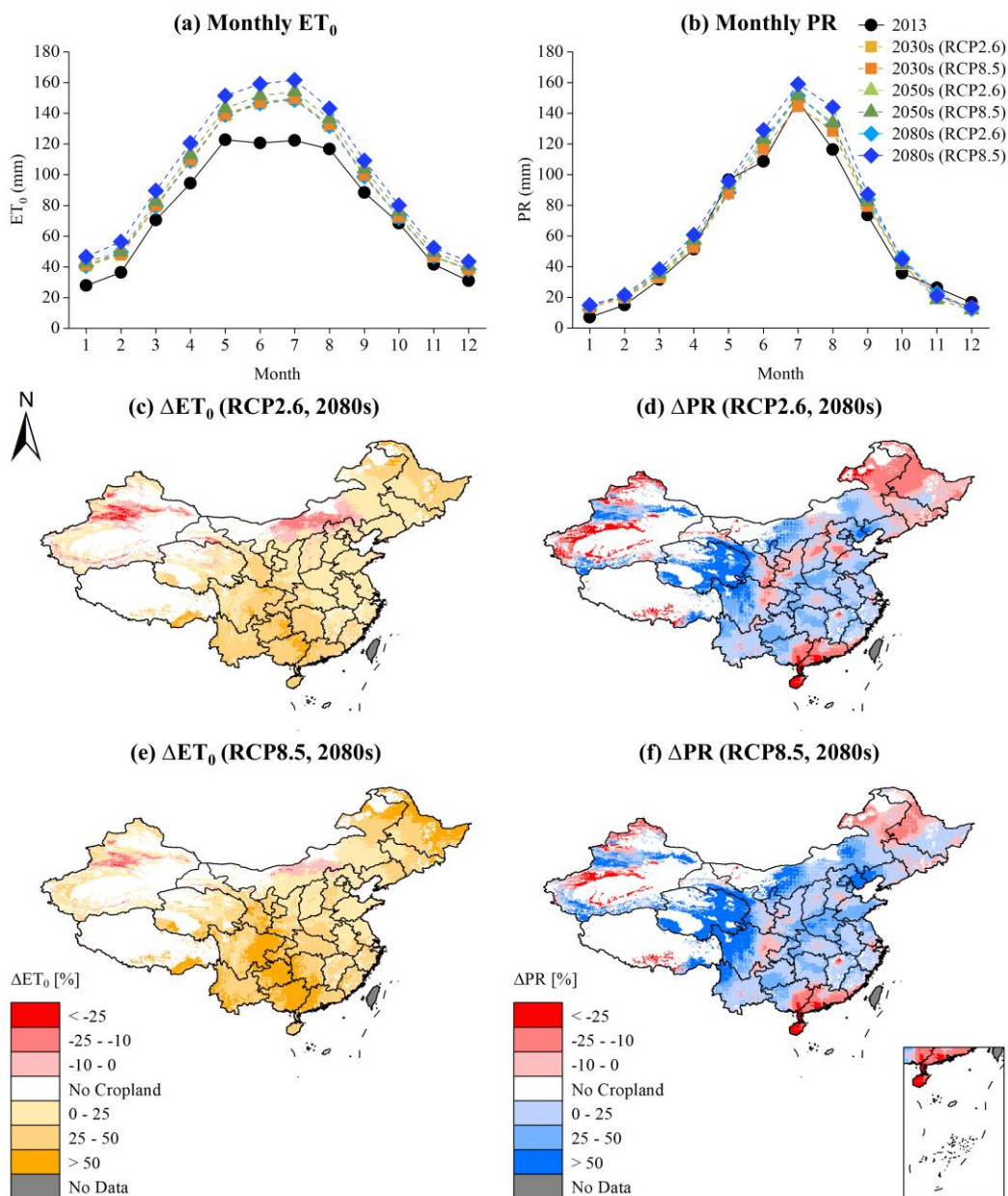
Figure 2. Future climate projections for the maize and wheat planted zones in China.

3.2 WFP distribution in the baseline year 2013

The national average WFP for wheat (1,008 m^3 t^{-1}) was higher than that for maize (813 m^3 t^{-1}) in the baseline year 2013.
The corresponding blue water footprint proportions were 37 % and 20 %, respectively. The reason for this discrepancy is that
maize is a C4 crop while wheat is a C3 crop. C4 crops have a relatively higher CO_2 fixation efficiency and faster photosynthetic

rate than C3 crops. Hence, maize can accumulate comparatively more yield than wheat under the same water consumption condition (Wang et al., 2012). Figure 3 shows that the high WFP_g value was distributed mainly in areas with relatively greater precipitation during crop growth, i.e., abundant green water resources. The main component of WFP is WFP_g. Therefore, the

185   high maize WFP was distributed mainly in Northwest (Fig. 3a) while the high wheat WFP was distributed mainly in Southwest and South Coast (Fig. 3b). Elevated ET_0 and insufficient precipitation can increase blue water consumption in food production. Thus, the high WFP_b value was distributed mainly in areas with uneven water and heat resource distributions during crop growth. The high maize WFP_b was distributed mainly in Northwest and East Coast (Fig. 3c) while that of wheat was distributed mainly in North China (Fig. 3d). In all grids, the proportions of WFP_b and WFP_g were up to 68 % (wheat in Xinjiang) (Table

190   S2) and 98 % (maize in Hainan) (Table S1), respectively.
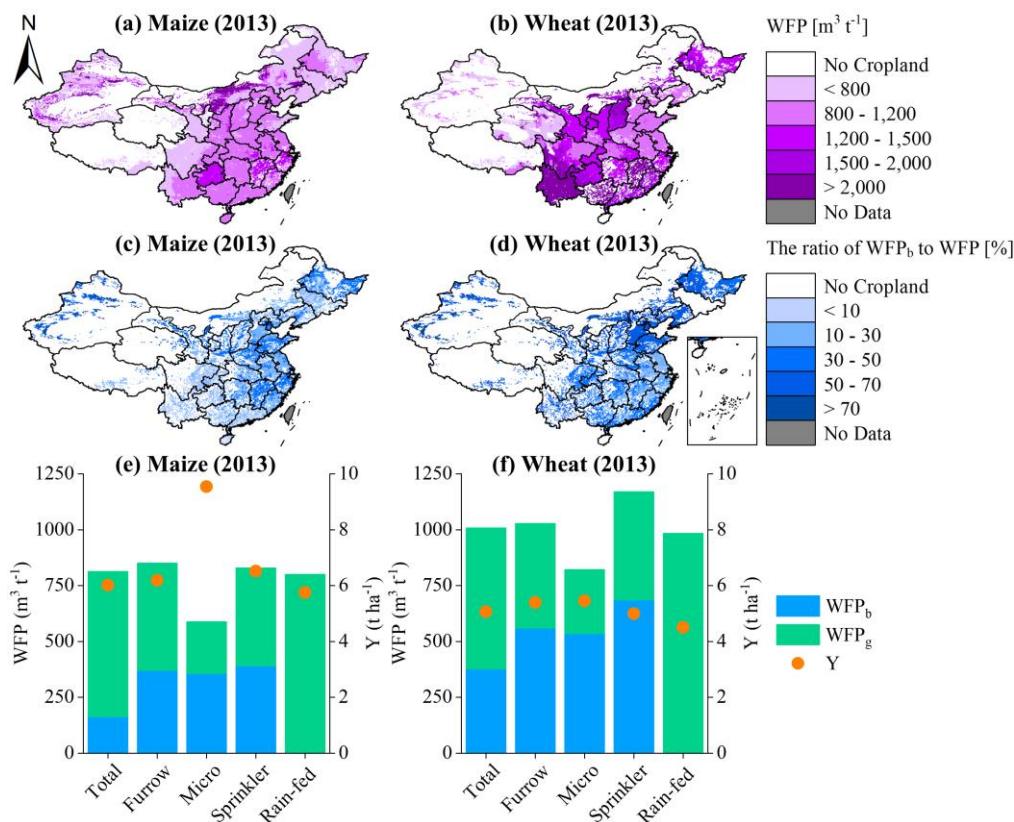
Figure 3. WFP of maize and wheat in China in 2013.

195   A comparison of rain-fed and irrigation techniques disclosed that the WFP of maize and wheat under furrow and sprinkler irrigation was higher than that under rain-fed in 2013. The WFP of micro-irrigated crops was lower than that of rain-fed crops. The WFP of maize (850 m^3 t^{-1}) and wheat (1,170 m^3 t^{-1}) was highest under furrow and sprinkler irrigation, respectively. For wheat under all three irrigation techniques, WFP_b was dominant (54–65 %). However, WFP_b for maize was only dominant

under micro irrigation (61 %). Micro-irrigated (9.55 t ha^{-1} for maize and 5.46 t ha^{-1} for wheat) and rain-fed (5.76 t ha^{-1} for
200   maize and 4.51 t ha^{-1} for wheat) crops had the highest and lowest yield, respectively, in 2013. The responses of maize yield to
rain-fed and various irrigation techniques were stronger than those of wheat yield (Fig. 3e, f).

3.3 Spatiotemporal responses of WFP to future climate change

Compared with the baseline year 2013 and at the national average level, maize WFP will increase under both RCP2.6 and
RCP8.5, by 17 % and 13 %, respectively, until the 2080s. The WFP of wheat will increase under RCP2.6 (by 12 % until the
205   2080s), but decrease by 12 % under RCP8.5 until the 2080s (Fig. 4a). The increases in CO_2 concentration and, by extension,
yield gain, will be lower under RCP2.6 than RCP8.5. During the same period, the increases in WFP under RCP2.6 will be 1–
3 % higher for maize and 2–10 % higher for wheat than those under RCP8.5. There will be relatively smaller differences in
CO_2 concentration between climate scenarios of the 2030s (431 ppm under RCP2.6 and 449 ppm under RCP8.5). Thus, the
differences in WFP between RCPs will be smaller before the 2030s and larger after the 2050s. The WFP of irrigated wheat
210   under RCP8.5 will decline in the second half of this century, by 3 % until the 2050s, and by 15 % until the 2080s. The increase
in WFP will be highest under rain-fed. The WFP of rain-fed maize and wheat under RCP2.6 will increase by 19 % and 24 %,
respectively, until the 2080s. By contrast, the WFP of irrigated maize and wheat under RCP2.6 will only increase by 13 % and
7 %, respectively, until the 2080s (Fig. 4a). A comparison of the various irrigation techniques demonstrated that the WFPs of
wheat and maize respond differently under the same scenario. The increase in WFP amplitude for maize will be highest under
215   furrow irrigation (14 % and 11 % under RCP2.6 and RCP8.5 until the 2080s, respectively) and lowest under micro irrigation
(5 % and 2 % under RCP2.6 and RCP8.5 until the 2080s, respectively). The WFP of sprinkler-irrigated wheat under RCP8.5
will decline by 1 % until the 2030s. The WFP of wheat under micro irrigation has the highest increase (9 % until the 2080s
under RCP2.6) and the lowest decrease (14 % until the 2080s under RCP8.5). The WFP of wheat under sprinkler irrigation
has the lowest increase (only 2 % until the 2080s under RCP2.6) and the highest decrease (19 % until the 2080s under RCP8.5)
220   (Fig. 4b).
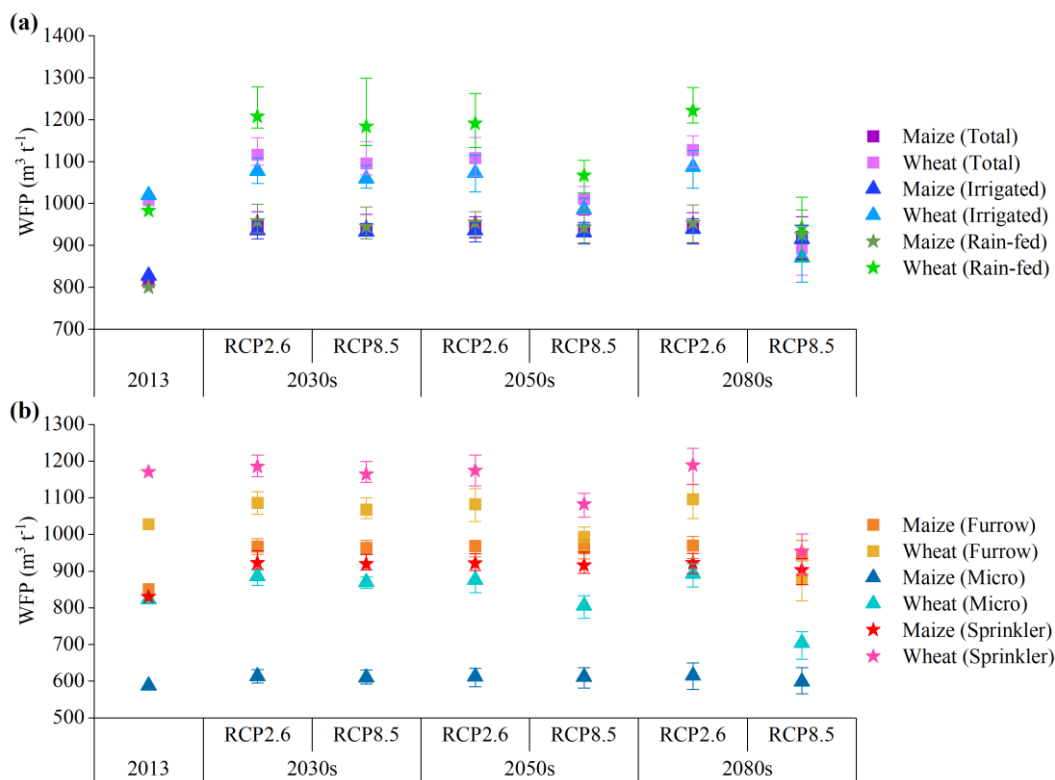
Figure 4. WFP of maize and wheat in 2013 and future year levels under various climate change scenarios in China.

The spatial distribution of the relative changes in maize and wheat WFP from 2013 to the 2080s shows regional differences. The WFP will increase for 90–93 % of all areas planted with maize (Fig. 5a, b). The WFP will increase for 78 % of all areas planted with wheat under RCP2.6 (Fig. 5c) and decrease for 81 % of all areas planted with wheat under RCP8.5 (Fig. 5d). Increases in ET_0 lead to increases in WFP while decreases in PR lead to increases in WFP_b (Fig. S6). Hence, the regions with relatively greater increases in WFP are distributed mainly where ET_0 strongly increases and PR slightly increases or even decreases. In Yunnan, maize WFP increases by 44 % and 38 % under RCP2.6 and RCP8.5, respectively. In Guangxi, wheat WFP increases by 50 % and 16 % under RCP2.6 and RCP8.5, respectively (Table S5). Comparison of rain-fed and various irrigation techniques reveals that WFP of each crop responds uniquely to latitudinal and longitudinal climate change under the same scenario. The responses of maize WFP to climate change with latitude are relatively consistent. It increases by 27–43 % at 19–26 °N and ~51 °N latitude and decreases at ~44 °N latitude. By contrast, the responses of WFP for rain-fed maize are more sensitive at ~40 °N and ~52 °N latitude. The responses of maize WFP vary widely within 74–100 °E longitude. The WFP of maize under rain-fed and furrow and sprinkler irrigation decline at 74–90 °E longitude. The increase in WFP for maize under rain-fed at 93–98 °E longitude is 3–51 % higher than the increase in WFP for maize under furrow and sprinkler irrigation. The WFP of micro-irrigated maize decreases at 74–95 °E longitude (Fig. 5a, b). The responses

of wheat WFP to climate change with latitude and longitude are relatively consistent. In certain areas, however, there are large

240 differences in wheat WFP between rain-fed and the three irrigation techniques. The WFP of wheat under rain-fed declines at

74–80 °E longitude and to a greater extent than the WFP of wheat under the three irrigation techniques at the same longitude

range. The increases in the WFP of wheat under rain-fed at ~93 °E and ~122 °E longitude and ~22 °N latitude are significantly

higher than the increases in WFP of wheat under the three irrigation techniques (Fig. 5c, d).
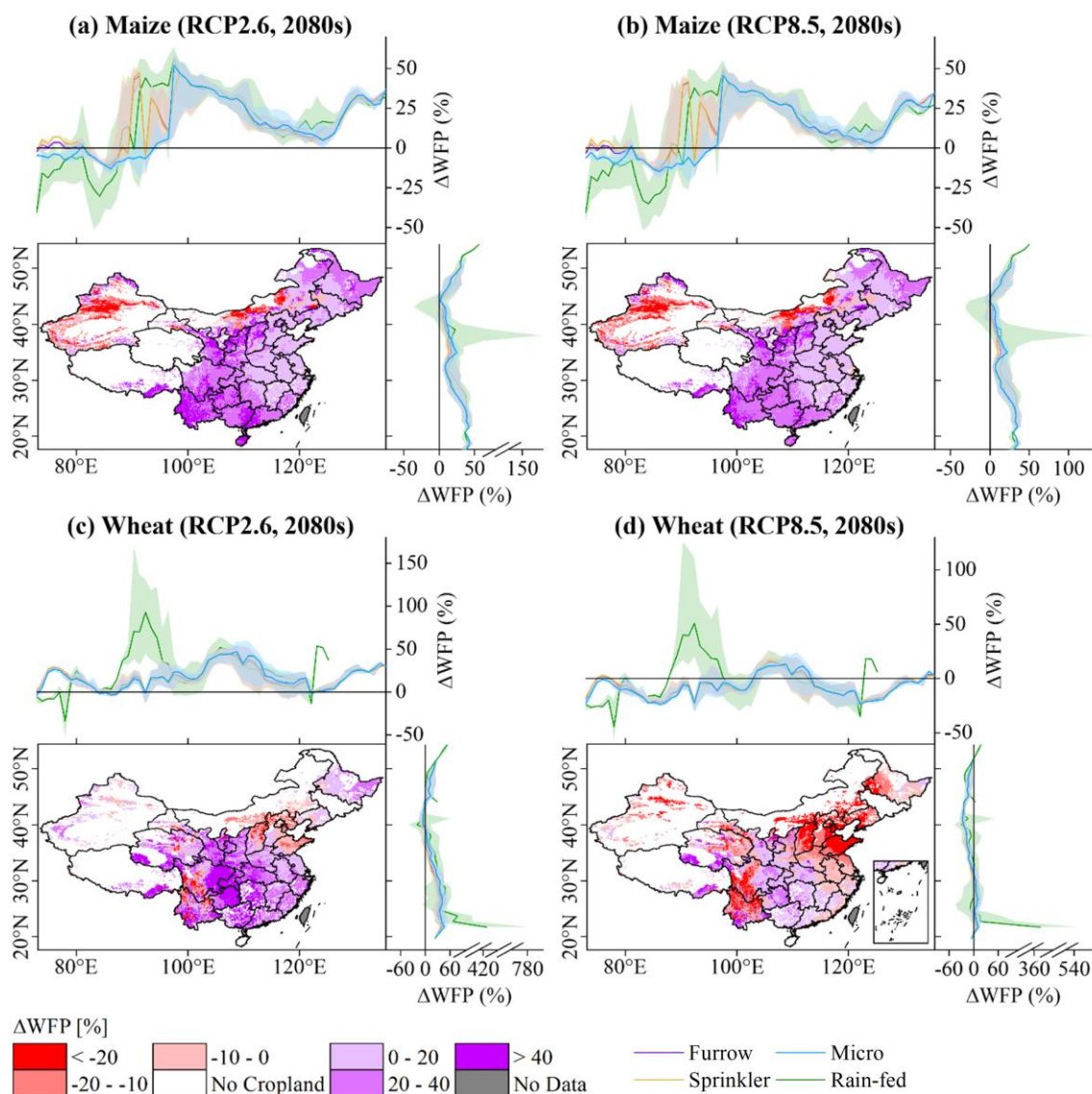
Figure 5. Spatial distributions in relative changes Δ (%) in WFP (bottom left panel) with longitudinal (top panel) and latitudinal (right

panel) changes under different irrigation techniques applied to both crops under two scenarios from 2013 to the 2080s.

WFP is determined both by crop yield (Y) and crop water use (CWU). We compared the relationships between the relative

250 changes in WFP (ΔWFP) and corresponding Y (ΔY) and CWU (ΔCWU) (Fig. 6). ΔWFP of maize and wheat under future climate change scenarios is inversely proportional to ΔY and directly proportional to ΔCWU. Nevertheless, ΔWFP is relatively more sensitive to ΔY. When ΔY is 25 %, ΔWFP of wheat under RCP2.6 and maize is approximately -25 % while ΔWFP of wheat under RCP8.5 is approximately -10 %. When ΔCWU is 25 %, ΔWFP of wheat under RCP2.6 and maize is ~20 % while ΔWFP of wheat under RCP8.5 is approximately -8 % (Fig. 6a, b). The responses of ΔWFP of maize are more sensitive to ΔY

255 and ΔCWU than those of wheat. The responses of ΔWFP of maize and wheat under RCP2.6 are more sensitive to ΔY and ΔCWU than those under RCP8.5. Comparison of rain-fed and various irrigation techniques revealed that the correlation between ΔWFP and ΔY is stronger for rain-fed crops. For rain-fed maize, R^2 can reach 0.55 (Fig. 6a). ΔWFP and ΔCWU are strongly correlated for irrigated crops. In fact, ΔWFP and ΔCWU are especially strongly correlated for crops under micro irrigation (R^2 can reach 0.98 for wheat) (Fig. 6b). We also compared the relationship between ΔWFP$_b$ and ΔCWU$_b$, and found

260 that it resembled that between ΔWFP and ΔCWU but more significant (Fig. 6c).
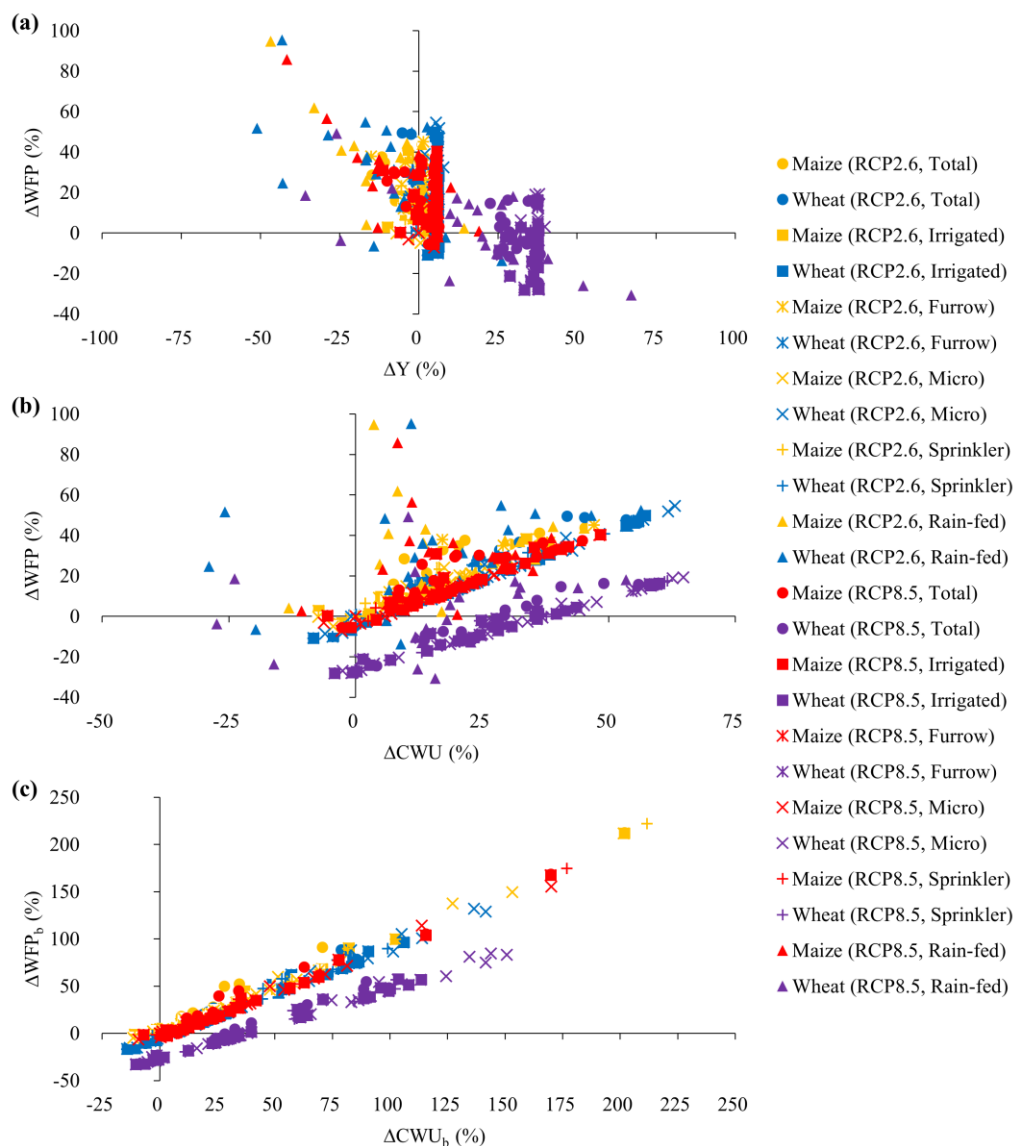
Figure 6. Relationships between relative changes Δ (%) in **(a)** Y and corresponding WFP, **(b)** CWU and corresponding WFP, and **(c)** CWU$_b$ and corresponding WFP$_b$ of two crops under RCP2.6 and RCP8.5 from 2013 to the 2080s.

3.4 Spatiotemporal WFP benchmarks responses to climate change

Table 2 shows WFP benchmarks of maize and wheat among various irrigation techniques and climate zones in 2013 and future year levels. WFP benchmarks of maize and wheat in the humid zone are 13–32 % higher than those in the arid zone, which is similar to Wang et al. (2019). In the same climate zone, WFP benchmarks of wheat are generally 2–35 % higher than those of maize. In the humid zone, however, the WFP benchmark for the 25th production percentile of maize will be 3 %

270 higher than that of wheat under RCP8.5 in the 2080s. In the arid zone, WFP benchmarks of rain-fed maize are 13–34 % higher than those of irrigated maize. In the humid zone of the future, WFP benchmarks of rain-fed wheat will be 2–7 % higher than those of irrigated wheat. In general, WFP benchmarks of sprinkler-irrigated crops are higher while those of micro-irrigated crops are lower. The differences in WFP benchmarks among various irrigation techniques are more significant in the arid zone. WFP benchmarks of the crops under micro irrigation are 30–38 % lower than those under sprinkler irrigation in the arid zone.

275 The difference in the humid zone is only 8–14 %. This is also consistent with Wang et al. (2019). In the humid zone, however, WFP benchmarks of maize under furrow irrigation are 7–21 % higher than those under sprinkler irrigation.

Table 2. WFP benchmarks ($m^3 t^{-1}$) of maize and wheat for different climate zones in 2013 and future year levels under two climate change scenarios in China.

Climate zones	Crop	Type	WFP ($m^3 t^{-1}$) at different production percentile[*]					
			20th			25th		
			2013	RCP2.6	RCP8.5	2013	RCP2.6	RCP8.5
Arid	Maize	Total	601	(577, 576, 580)	(589, 584, 566)	623	(661, 658, 655)	(655, 652, 634)
		Irrigated	522	(505, 504, 506)	(503, 503, 496)	548	(508, 507, 511)	(507, 509, 501)
		Furrow	618	(658, 658, 658)	(654, 654, 642)	654	(693, 693, 691)	(689, 687, 674)
		Micro	466	(455, 454, 456)	(456, 454, 440)	477	(459, 458, 460)	(458, 460, 446)
		Sprinkler	700	(727, 725, 723)	(722, 719, 708)	706	(729, 729, 726)	(724, 721, 710)
		Rain-fed	599	(661, 661, 662)	(652, 649, 630)	618	(682, 679, 671)	(672, 667, 652)
	Wheat	Total	753	(776, 764, 781)	(765, 707, 620)	768	(829, 816, 828)	(809, 756, 666)
		Irrigated	754	(776, 764, 781)	(765, 707, 620)	768	(830, 816, 829)	(810, 757, 666)
		Furrow	830	(850, 840, 850)	(830, 774, 680)	940	(885, 875, 887)	(868, 809, 712)
		Micro	648	(701, 690, 705)	(694, 643, 562)	670	(717, 705, 721)	(707, 654, 572)
		Sprinkler	1020	(1003, 998, 1007)	(989, 920, 811)	1032	(1034, 1028, 1038)	(1019, 948, 837)
		Rain-fed	692	(743, 734, 753)	(729, 692, 618)	692	(790, 772, 791)	(769, 737, 653)
Humid	Maize	Total	680	(761, 754, 752)	(756, 752, 739)	718	(813, 807, 807)	(809, 806, 785)
		Irrigated	743	(905, 905, 908)	(902, 900, 881)	782	(939, 939, 944)	(937, 936, 916)
		Furrow	762	(925, 926, 930)	(921, 921, 901)	801	(943, 942, 948)	(940, 939, 919)
		Micro	649	(709, 704, 707)	(694, 696, 683)	660	(734, 726, 732)	(721, 726, 708)
		Sprinkler	713	(770, 771, 768)	(764, 762, 750)	737	(813, 814, 812)	(808, 806, 793)
		Rain-fed	631	(712, 703, 707)	(710, 702, 678)	656	(744, 737, 737)	(740, 736, 716)
	Wheat	Total	873	(933, 932, 946)	(921, 851, 752)	887	(944, 942, 957)	(931, 860, 760)
		Irrigated	887	(914, 914, 924)	(900, 841, 744)	897	(925, 926, 937)	(912, 849, 752)
		Furrow	887	(914, 914, 925)	(901, 841, 744)	896	(925, 927, 937)	(913, 849, 752)
		Micro	820	(821, 826, 838)	(804, 753, 665)	833	(830, 839, 849)	(812, 759, 671)
		Sprinkler	933	(949, 944, 955)	(936, 872, 770)	946	(958, 953, 964)	(944, 880, 777)
		Rain-fed	812	(973, 958, 984)	(950, 863, 757)	831	(989, 973, 998)	(964, 877, 763)

[*]The three numbers in brackets are the values of 2030s, 2050s and 2080s.

280

Compared with the baseline year 2013, the changes in maize and wheat WFP benchmarks under future climate change scenarios are similar to the changes in WFP. However, the WFP benchmark for the 20th production percentile of maize will decline by 2–6 % in the arid zone. WFP benchmarks of wheat under RCP8.5 will decrease by 2–6 % and 13–18 % until the 2050s and the 2080s, respectively. The increasing range of the WFP benchmark for the 25th production percentile of maize is 7–8 % higher in the humid zone than that in the arid zone. The increasing range of the WFP benchmark for the 20th production percentile of wheat is 4–5 % higher in the humid zone than that in the arid zone. WFP benchmarks of maize and wheat increase to a greater extent under RCP2.6 but decrease to a greater extent under RCP8.5. WFP benchmarks of rain-fed crops increase more than those of irrigated crops in the same climate zone. Nevertheless, the increase in WFP benchmarks is 7–11 % lower for rain-fed than irrigated maize in the humid zone. WFP benchmarks of maize and wheat generally increase relatively more under furrow irrigation and comparatively less under sprinkler irrigation. However, under RCP2.6, the growth rate of the WFP benchmark for the 20th production percentile of wheat is 5–6 % higher under micro irrigation than that under furrow irrigation in the arid zone. The increase in the WFP benchmark for the 20th production percentile of wheat is 0.19–2 % higher under sprinkler irrigation than that under micro irrigation in the humid zone (Table 2).

Figure 7 shows the spatial distribution of the relative changes in WFP of maize and wheat compared with the benchmark for the 25th production percentile in 2013 and the 2080s. In 2013, the WFP for 81 % and 79 % of the maize and wheat planted areas, respectively, was higher than its benchmark. The maize planted areas with WFP below the benchmark were distributed mainly in Xinjiang in the arid zone and northeast Inner Mongolia in the humid zone (Fig. 7a). The wheat planted areas with WFP below the benchmark were distributed mainly in Xinjiang in the arid zone and Qinghai (Fig. 7d). Under future climate change scenarios, the maize and wheat planted areas with WFP below the benchmark will slightly decrease in the 2080s. These areas are mainly distributed in Heilongjiang, Tibet, southern Gansu and Sichuan in the humid zone for maize, and Henan, Tibet in the humid zone and Qinghai for wheat. This is because that the annual ET_0 will increase relatively faster in Heilongjiang and Tibet which will, in turn, lead to a greater increase in WFP_b. The annual PR in other regions will significantly increase which will result in a greater increase in WFP_g. Maize and wheat planted areas under RCP8.5 with WFP below the benchmark will decrease by 5 % and 4 %, respectively, until the 2080s.
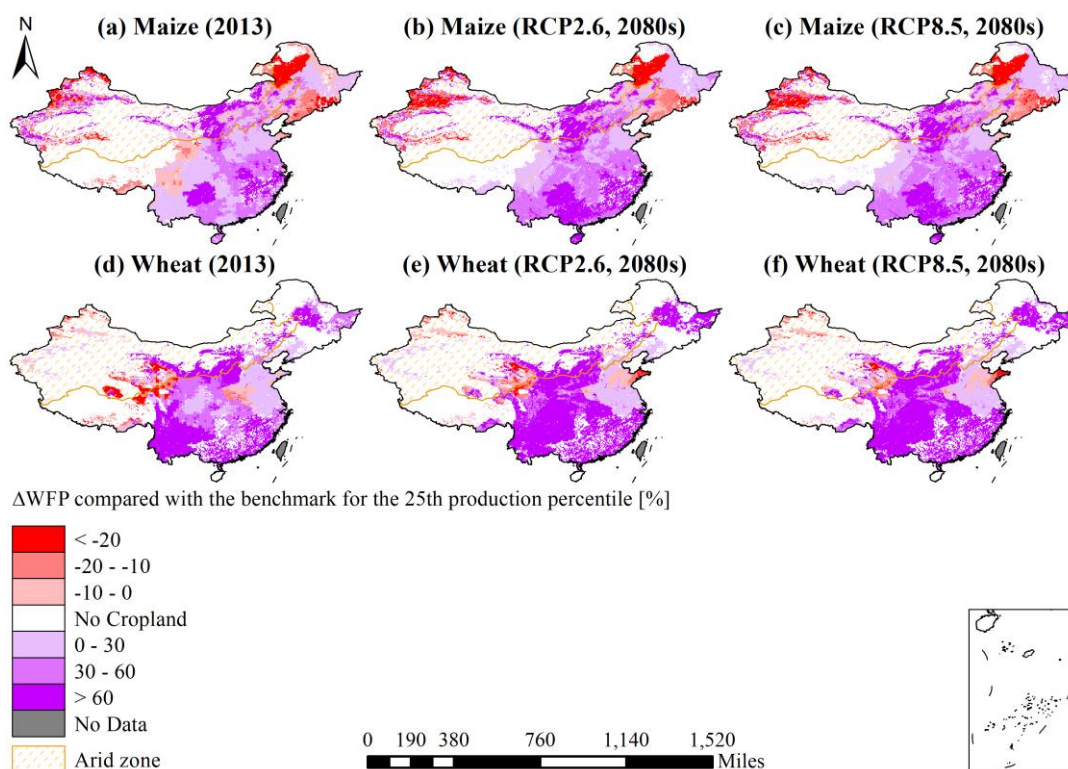
Figure 7. Relative changes Δ (%) in WFP of maize and wheat compared with the benchmark for the 25th production percentile in 2013 and the 2080s under RCP2.6 and RCP8.5 in different climate zones of China.

310 **3.5 Discussion**

This study analysed and compared the WFP and WFP benchmarks responses of wheat and maize under rain-fed and various irrigation conditions and forecasted their responses to future climate change scenarios in China. Under the background that the annual ET_0 and PR will both increase but ET_0 will increase faster, maize WFP will increase under both two RCPs. Wheat WFP will increase under RCP2.6 but decrease under RCP8.5 until the 2080s. Rain-fed crops have higher ranges of 315 increasing WFP, which is consistent with Rosa et al. (2020). The increasing ranges of maize and wheat WFP are lowest under micro irrigation and sprinkler irrigation, respectively. Therefore, the implementation of water-saving irrigation techniques (micro and sprinkler irrigation) might help mitigate the adverse effects of future climate change on agriculture, which is in line with Dai et al. (2020). Under future climate change, WFP benchmarks will be modified in a manner resembling that for WFP. However, the former changes will not be as significant as the latter in spatial distribution.

320

In 2013, WFP of maize was lower than that of wheat. Nevertheless, maize WFP is expected to increase more rapidly than wheat WFP under future climate change scenarios. C4 crops such as maize have higher photosynthetic rates than C3 crops such as wheat. However, the former are less sensitive to elevated atmospheric CO_2 than the latter (Bowes, 1993). Hence, while
325 maize yield is higher than wheat yield, the former increases less than the latter. We compared current results against those of previous studies in Table 3. The differences we determined for the relative changes in maize and wheat WFP between years and RCPs resembled those reported by Zhuo et al. (2016c). However, these authors also considered other factors such as harvested crop area, technology, diet, and population that could partially offset the adverse effects of future climate change. Therefore, maize and wheat WFP will decline in the future according to Zhuo et al. (2016c). Fader et al. (2010) studied relative
330 global-scale changes in maize WFP for the year 2050. Their analysis was conducted in the opposite direction of that of the present study on China. Moreover, the two studies differed in terms of climate scenario, research area, and crop model. Winter wheat WFP in Germany and Italy will decline by 2050 according to Garofalo et al. (2019). Nevertheless, our research showed that winter wheat WFP will increase in China by 2050. The crop water use in Germany and Italy changes more slightly than that in China. However, our observed differences in the relative changes in WFP between RCPs were consistent with those of
335 Garofalo et al. (2019), namely, under RCP8.5, WFP will either decrease more or increase less.

Table 3. Comparison of the results between current and previous studies.

Reference	Year	Study case	Scenario	Relative changes in WFP (%)
Zhuo et al. (2016c)	2030	China Maize	RCP2.6 / RCP8.5	-38--32 / -10-0
		China Wheat		-25--17 / -20--11
	2050	China Maize		-51--43 / -22--8
		China Wheat		-36--27 / -38--27
Current study	2030s (2020–2049)	China Maize	RCP2.6 / RCP8.5	17 / 16
		China Wheat		11 / 9
	2050s (2040–2069)	China Maize		16 / 15
		China Wheat		10 / 0.20
Fader et al. (2010)	2041–2070	Global Maize	SRES A2	-0.44--0.35
Current study	2050s (2040–2069)	China Maize	RCP2.6 / RCP8.5	16 / 15
Garofalo et al. (2019)	2050	Germany Winter wheat	RCP4.5 / RCP8.5	-24 / -26
		Italy Winter wheat		-5 / -6
Current study	2050s (2040–2069)	China Winter wheat	RCP2.6 / RCP8.5	10 / 0.60

In the future, the spatial distributions of maize and wheat WFP will change considerably. By contrast, the spatial
340 distributions of WFP benchmarks will change relatively little. This phenomenon is comparatively more pronounced in areas with limited agricultural development. In 2013, Guizhou and Guangxi had the highest maize and wheat WFP (1,317 m³ t⁻¹ and 3,720 m³ t⁻¹, respectively) (Table S1, S2). In the humid zone, maize WFP in Guizhou and wheat WFP in Guangxi will increase by 37 % and 50 %, respectively, under RCP2.6 and by 33 % and 16 %, respectively, under RCP8.5 until the 2080s (Table S5). Nevertheless, the WFP benchmarks for the 25th production percentile of maize and wheat in the humid zone will only increase
345 by 12 % and 8 %, respectively, under RCP2.6 and increase by 9 % and decrease by 14 %, respectively, under RCP8.5. These

areas will nonetheless have great potential for agricultural water conservation in the future. If maize and wheat WFP in various regions of China can be reduced to the benchmark for the 25th production percentile, the total CWU can be reduced by 45–66 billion m^3 (~14–17 %). Rain-fed agriculture can save 27–40 billion m^3 (~18–22 %) water which is more than that conserved by irrigation. In irrigated agriculture, furrow irrigation has a comparatively high water-saving potential (17–22 billion m^3;

350 ~11–12 %). To optimise the agricultural water-saving potential in China, we must either reduce WFP or prevent it from increasing either by enhancing crop yield or decreasing CWU. However, this goal can only be realised with the support of relevant policies and management practices. The annual PR is relatively low and the ET_0 is relatively high in North China. Shortage of water for agriculture is a major bottleneck in the development of local agriculture there. However, furrow irrigation is mainly applied in these areas (Fig. S3). Hence, irrigation water use efficiency is low and WFP_b is high. High-efficiency,

355 water-saving micro irrigation and sprinkler irrigation could replace furrow irrigation there so that CWU and WFP are decreased. The planted areas in the South have abundant precipitation but limited distribution (Fig. S2) and high WFP (Fig. 3a, b). WFP can be mitigated by implementing ground cover techniques (ex. straw return, mulch) to reduce soil evaporation and by improving farmer skills. WFP can also be reduced by optimizing crops planting structure. Crops and varieties best adapted to local climate conditions and climate change can lower irrigation requirements and reduce WFP.

360 In order to make climate models comparable and promote the development of them, The World Climate Research Program (WCRP) has developed and promoted the CMIP since 1995 (Meehl et al., 1997, 2000). Its current iteration is CMIP Phase 6 (CMIP6) which will be used in the forthcoming Intergovernmental Panel on Climate Change's Sixth Assessment Report (IPCC AR6). GCMs and their associated research results based on CMIP5 provided vital support for IPCC's Fifth Assessment Report (IPCC AR5). CMIP5 proposed four RCP scenarios (RCP2.6, RCP4.5, RCP6.0, and RCP8.5) by

365 considering greenhouse gas (GHG) emissions and concentrations, atmospheric pollutant concentrations, and land use in the 21st century (Moss et al., 2008). However, no specific socio-economic assumptions were made. The Scenario Model Intercomparison Project (ScenarioMIP) as the primary activity within CMIP6 will provide a series of new climate scenarios that consider social factors related to climate change adaptation and impacts. They will be based on the combined application of shared socioeconomic pathways (SSPs) and RCPs and will compensate for the shortcomings of the RCPs in CMIP5 (O'Neill

370 et al., 2016). The climate models in CMIP5 and CMIP6 can both effectively simulate changes in potential evapotranspiration (Liu et al., 2020) and precipitation (Müller et al., 2021) in most parts of the world. Müller et al. (2021) reported that CMIP5 and CMIP6 simulate increasing trends in temperature in a similar fashion. Nevertheless, the simulation generated by CMIP6 is higher than that by CMIP5. Notwithstanding, CMIP5 and CMIP6 are reasonably consistent and similar in terms of their abilities to predict future climate changes. This study focused on the responses of crop production to future climate change. It

375 considered mainly the influences of GHG emission- and concentration-driven climate change and excluded the influences of alterations in socioeconomic development. For these reasons, we implemented CMIP5 in our research here.

The sources of uncertainty in research on the responses of crop production to climate change include GCMs, climate scenarios, crop models, and their interactions (Wang et al., 2020). Semenov and Stratonovitch (2010) proposed that the use of multiple GCMs can reduce the uncertainty associated with them. We selected three GCMs each for wet and dry climate outputs

380   to encompass a broad climate prediction scenario. To project the future climate change trends of China objectively and comprehensively, we selected two extreme RCPs, namely, RCP2.6 and RCP8.5. Wang et al. (2020) suggested that crop models are the main source of uncertainty in predicting wheat yield in China under future climate change. The application of various crop models and parameter settings inevitably lead to different yield forecasts (Asseng et al., 2013). Hence, the use of AquaCrop alone may introduce uncertainty into WFP forecasting.

385   The present study had certain limitations in terms of the assumptions it made for the simulation. First, we assumed that the crop parameters (such as planting calendar, HI, Zx, and so on) for each crop under the identical planting mode (irrigated or rain-fed) were constant on a spatiotemporal scale. Yoon and Choi (2020) proposed that future increases in temperature and precipitation might shorten the crop growth period. Xiao et al. (2020) indicated that the winter wheat and summer maize growing periods will be lengthened and shortened, respectively, under future climate change. However, we did not consider

390   future changes in the crop growth period. Second, we assumed a constant soil surface moisture rate for each grid under the various irrigation techniques. Third, it was assumed that the observed changes in the planted areas in 2013 were based on the 2000 raster database and ignored planted areas migration. Finally, we assumed that the maize and wheat planted areas will not change in the future and would remain consistent with baseline year 2013. Thus, we did not consider future development of cultivated lands.

395   The core content of this study was to quantify the responses of maize and wheat WFP and WFP benchmarks to future climate change under various irrigation techniques. To this end, we coupled the AquaCrop model to the GCMs outputs. Future research must improve the accuracy of the crop model simulation and reduce the uncertainty of climate prediction associated with using different GCMs. Moreover, this study only considered future climate change scenarios. Future investigations should also consider the influence of changes in technological development, land use, planting modes, and so on.

4 Conclusions

This study explored the responses of maize and wheat WFP accounting and benchmarking to future climate change in China. The crops were subjected to various irrigation techniques. The year 2013 was the baseline and WFP and its benchmarks were quantified for each crop under rain-fed and irrigation (furrow, micro, and sprinkler) managements in the 2030s, 2050s, and 2080s under RCP2.6 and RCP8.5 at a 5-arc grid scale. AquaCrop model coupled with six GCMs in CMIP5 was used. The

405   results show that: (1) Compared with 2013, the annual ET_0 and PR in the maize and wheat planted areas of China will both increase but the former will increase faster than the latter. (2) Maize WFP will increase under both RCP2.6 and RCP8.5, by 17 % and 13 %, respectively, until the 2080s. Wheat WFP will increase under RCP2.6 (by 12 % until the 2080s), but decrease by 12 % under RCP8.5 until the 2080s. Rain-fed crops are more vulnerable to the adverse impacts of future climate change and their WFP increases to a greater extent than that of irrigated crops. Micro irrigation and sprinkler irrigation result in the

410   lowest increases in WFP for maize and wheat, respectively. Hence, these water-saving irrigation practices effectively mitigate the negative impact of climate change. (3) Within different climate zones and under various irrigation techniques, there will

be significant differences in the responses of WFP benchmarks to future climate change. The changes in WFP and its benchmarks will be similar in response to future climate change. The rate of increase in WFP benchmarks for sprinkler-irrigated crops will generally be lower than those for rain-fed, micro-irrigated, and furrow-irrigated crops within the same climate zone. However, the change in the spatial distribution of WFP benchmarks will not be as significant as that of WFP itself. Moreover, the differences in the spatial distributions of WFP and its benchmarks will be more pronounced in regions with low agricultural development. Additionally, this study demonstrated that agricultural water can be effectively conserved in China. To this end, management practices should include water-saving irrigation, ground cover such as mulching and straw return, improvement of farmer skills, optimizing crops planting structure. In this manner, the agricultural water-saving potential of China can be maximised and sustainable water supply and food production security can be established and maintained under future climate change.

Data availability. Data sources are listed in Sect. 2.4. Data generated in this paper are available by contacting La Zhuo.

Competing interests. The authors declare that they have no conflict of interest.

Acknowledgements

The study is financially supported by the Program for Cultivating Outstanding Talents on Agriculture, Ministry of Agriculture and Rural Affairs, People's Republic of China [13210321], and the National Natural Science Foundation of China Grants [51809215].

References

Ahmadi, M., Etedali, H. R., and Elbeltagi, A.: Evaluation of the effect of climate change on maize water footprint under RCPs scenarios in Qazvin plain, Iran, Agr. Water Manage., 254, 106969, https://doi.org/10.1016/j.agwat.2021.106969, 2021.

Allen, R. G., Pereira, L. S., Raes, D., and Smith, M.: Crop evapotranspiration-Guidelines for computing crop water requirements-FAO Irrigation and drainage paper 56, 300, FAO, Rome, Italy, 1998.

Arora, V. K., Scinocca, J. F., Boer, G. J., Christian, J. R., Denman, K. L., Flato, G. M., Kharin, V. V., Lee, W. G., and Merryfield, W. J.: Carbon emission limits required to satisfy future representative concentration pathways of greenhouse gases, Geophys. Res. Lett., 38, 387–404, https://doi.org/10.1029/2010GL046270, 2011.

Arunrat, N., Pumijumnong, N., Sereenonchai, S., Chareonwong, U., and Wang, C.: Assessment of climate change impact on rice yield and water footprint of large-scale and individual farming in Thailand, Sci. Total Environ., 726, 137864, https://doi.org/10.1016/j.scitotenv.2020.137864, 2020.

Asseng, S., Ewert, F., Rosenzweig, C., Jones, J. W., Hatfield, J. L., Ruane, A. C., Boote, K. J., Thorburn, P. J., Rötter, R. P., Cammarano, D., Brisson, N., Basso, B., Martre, P., Aggarwal, P. K., Angulo, C., Bertuzzi, P., Biernath, C., Challinor, A. J., Doltra, J., Gayler, S., Goldberg, R., Grant, R., Heng, L., Hooker, J., Hunt, L. A., Ingwersen, J., Izaurralde, R. C., Kersebaum, K. C., Müller, C., Naresh Kumar, C., Nendel, C., O'Leary, G., Olesen, J. E., Osborne, T. M., Palosuo, T., Priesack, E., Ripoche, D., Semenov, M. A., Shcherbak, I., Steduto, P., Stöckle, C., Stratonovitch, P., Streck, T., Supit, I., Tao, F., Travasso, M., Waha, K., Wallach, D., White, J. W., Williams, J. R., and Wolf, J.: Uncertainty in simulating wheat yields under climate change, Nat. Clim. Chang., 3, 827–832, https://doi.org/10.1038/nclimate1916, 2013.

Batjes, N.: ISRIC-WISE Derived Soil Properties on a 5 by 5 Arc-Minutes Global Grid (Ver. 1.2), ISRIC, Wageningen, The Netherlands, available at: https://www.isric.org, 2012.

Bowes, G.: Facing the Inevitable: Plants and Increasing Atmospheric CO2, Annu. Rev. Plant Phys. Plant Mol. Biol., 44, 309–332, https://doi.org/10.1146/annurev.pp.44.060193.001521, 1993.

CCAFS: CCAFS-Climate Statistically Downscaled Delta Method data, Climate Change, Agriculture and Food Security, available at: www.ccafs-climate.org, 2015.

CEDA: Climatic Research Unit (CRU) time-series datasets of variations in climate with variations in other phenomena, NCAS British Atmospheric Data Centre, date of citation, available at: http://catalogue.ceda.ac.uk/uuid, 2018.

Chukalla, A. D., Krol, M. S., and Hoekstra, A. Y.: Green and blue water footprint reduction in irrigated agriculture: Effect of irrigation techniques irrigation strategies and mulching, Hydrol. Earth Syst. Sci., 19, 4877–4891, https://doi.org/10.5194/hess-19-4877-2015, 2015.

Dai, C., Qin, X. S., Lu, W. T., and Huang, Y.: Assessing adaptation measures on agricultural water productivity under climate change: A case study of Huai River Basin, China, Sci. Total Environ., 721, 137777, https://doi.org/10.1016/j.scitotenv.2020.137777, 2020.

Delworth, T. L., Broccoli, A. J., Rosati, A., Stouffer, R. J., Balaji, V., Beesley, J. A., Cooke, W. F., Dixon, K. W., Dunne, J., Dunne, K. A., Durachta, J. W., Findell, K. L., Ginoux, P., Gnanadesikan, A., Gordon, C. T., Griffies, S. M., Gudgel, R., Harrison, M. J., Held, I. M., Hemler, R. S., Horowitz, L. W., Klein, S. A., Knutson, T. R., Kushner, P. J., Langenhorst, A. R., Lee, H. C., Lin, S. J., Lu, J., Malyshev, S. L., Milly, P. C. D., Ramaswamy, V., Russell, J., Schwarzkopf, M. D., Shevliakova, E., Sirutis, J. J., Spelman, M. J., Stern, W. F., Winton, M., Wittenberg, A. T., Wyman, B., Zeng, F., and Zhang, R.: GFDL's CM2 Global Coupled Climate Models. Part I: Formulation and Simulation Characteristics, J. Clim., 19, 643–674, https://doi.org/10.1175/JCLI3629.1, 2006.

Dijkshoorn, J. A., Engelen, V. W. P. V., and Huting, J. R. M.: Soil and landform properties for LADA partner countries (Argentina, China, Cuba, Senegal, South Africa and Tunisia), ISRIC–World Soil Information and FAO, Wageningen, the Netherlands, available at: https://www.isric.org/, https://doi.org/10.13031/2013.42676, 2008.

Donner, L. J., Wyman, B. L., Hemler, R. S., Horowitz, L. W., Ming, Y., Zhao, M., Golaz, J. C., Ginoux, P., Lin, S. J., Schwarzkopf, M. D., Austin, J., Alaka, G., Cooke, W. F., Delworth, T. L., Freidenreich, S. M., Gordon, C. T., Griffies, S. M., Held, I. M., Hurlin, W. J., Klein, S. A., Knutson, T. R., Langenhorst, A. R., Lee, H. C., Lin, Y., Magi, B. I.,

475   Malyshev, S. L., Milly, P. C. D., Naik, V., Nath, M. J., Pincus, R., Ploshay, J. J., Ramaswamy, V., Seman, C. J.,
        Shevliakova, E., Sirutis, J. J., Stern, W. F., Stouffer, R. J., Wilson, R. J., Winton, M., Wittenberg, A. T., and Zeng, F.:
        The Dynamical Core, Physical Parameterizations, and Basic Simulation Characteristics of the Atmospheric Component
        AM3 of the GFDL Global Coupled Model CM3, J. Clim., 24, 3484–3519, https://doi.org/10.1175/2011JCLI3955.1, 2011.

        Dufresne, J. L., Foujols, M. A., Denvil, S., Caubel, A., Marti, O., Aumont, O., Balkanski, Y., Bekki, S., Bellenger, H., Benshila,
480   R., Bony, S., Bopp, L., Braconnot, P., Brockmann, P., Cadule, P., Cheruy, F., Codron, F., Cozic, A., Cugnet, D., Noblet,
        N. D., Duvel, J. P., Ethé, C., Fairhead, L., Fichefet, T., Flavoni, S., Friedlingstein, P., Grandpeix, J. Y., Guez, L., Guilyardi,
        E., Hauglustaine, D., Hourdin, F., Idelkadi, A., Ghattas, J., Joussaume, S., Kageyama, M., Krinner, G., Labetoulle, S.,
        Lahellec, A., Lefebvre, M. P., Lefevre, F., Levy, C., Li, Z. X., Lloyd, J., Lott, F., Madec, G., Mancip, M., Marchand, M.,
        Masson, S., Meurdesoif, Y., Mignot, J., Musat, I., Parouty, S., Polcher, J., Rio, C., Schulz, M., Swingedouw, D., Szopa,
485   S., Talandier, C., Terray, P., Viovy, N., and Vuichard, N.: Climate change projections using the IPSL-CM5 Earth System
        Model: from CMIP3 to CMIP5, Clim. Dyn., 40, 2123–2165, https://doi.org/10.1007/s00382-012-1636-1, 2013.

        Fader, M., Rost, S., Müller, C., Bondeau, A., and Gerten, D.: Virtual water content of temperate cereals and maize: Present
        and potential future patterns, J. Hydrol., 384, 218–231, https://doi.org/10.1016/j.jhydrol.2009.12.011, 2010.

        FAO: FAOSTAT on-line database, Food and Agriculture Organization of the United Nation, Rome, Italy, available at:
490   http://www.fao.org/faostat/en/#data/QC, 2021.

        Garofalo, P., Ventrella, D., Kersebaum, K. C., Gobin, A., Trnka, M., Giglio, L., Dubrovský, M., and Castellini, M.: Water
        footprint of winter wheat under climate change: Trends and uncertainties associated to the ensemble of crop models, Sci.
        Total Environ., 658, 1186–1208, https://doi.org/10.1016/j.scitotenv.2018.12.279, 2019.

        Harris, I., Jones, P. D., Osborn, T. J., and Lister, D. H: Updated high-resolution grids of monthly climatic observations - the
495   CRU TS3.10 Dataset, Int. J. Climatol., 34, 623–642, https://doi.org/10.1002/joc.3711, 2014.

        Hatfield, J. L. and Dold, C.: Water-Use Efficiency: Advances and Challenges in a Changing Climate, Front. Plant Sci., 10,
        103, https://doi.org/10.3389/fpls.2019.00103, 2019.

        Hoekstra, A. Y. (ed.): Virtual water trade: Proceedings of the International Expert Meeting on Virtual Water Trade, Delft, the
        Netherlands, 12–13 December 2002, Value of Water Research Report Series No. 12, UNESCO-IHE, Delft, The
500   Netherlands, 2003.

        Hoekstra, A. Y.: The water footprint of modern consumer society, Routledge, London, UK, 208 pp, 2013.

        Hoekstra, A. Y.: Sustainable, efficient, and equitable water use: the three pillars under wise freshwater allocation, Wiley
        Interdisc. Rev. Water, 1, 31–40, https://doi.org/10.1002/wat2.1000, 2013.

        Hoekstra, A. Y., Chapagain, A. K., Aldaya, M. M., and Mekonnen, M. M.: The Water Footprint Assessment Manual: Setting
505   the Global Standard, Earthscan, London, UK, 2011.

        Hurrell, J. W., Holland, M. M., Gent, P. R., Ghan, S., Kay, J. E., Kushner, P. J., Lamarque, J. F., Large, W. G., Lawrence, D.,
        Lindsay, K., Lipscomb, W. H., Long, M. C., Mahowald, M., Marsh, D. R., Neale, R. B., Rasch, P., Vavrus, S., Vertenstein,
        M., Bader, D., Collins, W. D., Hack, J. J., Kiehl, J., and Marshall, S.: The Community Earth System Model: A Framework

for Collaborative Research, Bull. Am. Meteorol. Soc., 94, 1339–1360, https://doi.org/10.1175/BAMS-D-12-00121.1,
510   2013.

IPCC: Summary for Policymakers. In: Climate Change 2021: The Physical Science Basis. Contribution of Working Group I
to the Sixth Assessment Report of the Intergovernmental Panel on Climate Change, edited by: Masson-Delmotte, V.,
Zhai, P., Pirani, A., Connors, S. L., Péan, C., Berger, S., Caud, N., Chen, Y., Goldfarb, L., Gomis, M. L., Huang, M.,
Leitzell, K., Lonnoy, E., Matthews, J. B. R., Maycock, T. K., Waterfield, T., Yelekçi, O., Yu, R., and Zhou, B., Cambridge
515   University Press, In Press, 2021.

Jans, Y., Bloh, W. V., Schaphoff, S., and Müller, C.: Global cotton production under climate change – Implications for yield
and water consumption, Hydrol. Earth Syst. Sci., 25, 2027–2044, https://doi.org/10.5194/hess-25-2027-2021, 2021.

Kappelle, M.: WMO Statement on the State of the Global Climate in 2019, World Meteorological Organization, Geneva,
Switzerland, 2020.

520   Konapala, G., Mishra, A. K., Wada, Y., and Mann, M. E.: Climate change will affect global water availability through
compounding changes in seasonal precipitation and evaporation, Nat. Commun., 11, 3044,
https://doi.org/10.1038/s41467-020-16757-w, 2020.

Liu, X., Li, C., Zhao, T., and Han, L.: Future changes of global potential evapotranspiration simulated from CMIP5 to CMIP6
models, Atmos. Oceanic Sci Lett., 13, 568–575, https://doi.org/10.1080/16742834.2020.1824983, 2020.

525   Lobell, D. B. and Gourdji, S. M.: The influence of climate change on global crop productivity, Plant Physiol., 160, 1686–1697,
https://doi.org/10.1104/pp.112.208298, 2012.

Mali, S. S., Shirsath, P. B., and Islam, A.: A high-resolution assessment of climate change impact on water footprints of cereal
production in India, Sci. Rep., 11, 8715, https://doi.org/10.1038/s41598-021-88223-6, 2021.

Meehl, G. A., Boer, G. J., Covey, C., Latif, M., and Stouffer, R. J.: Intercomparison makes for a better climate model, Eos.
530   Trans. Amer. Geophys. Union, 78, 445–451, https://doi.org/10.1029/97EO00276, 1997.

Meehl, G. A., Boer, G. J., Covey, C., Latif, M., and Stouffer, R. J.: The Coupled Model Intercomparison Project (CMIP), Bull.
Am. Meteorol. Soc., 81, 313–318, https://doi.org/10.1175/1520-0477(2000)081<0313:TCMIPC>2.3.CO;2, 2000.

Mekonnen, M. M. and Hoekstra, A. Y.: The green, blue and grey water footprint of crops and derived crop products, Hydrol.
Earth Syst. Sci., 15, 1577-1600, doi:10.5194/hess-15-1577-2011, 2011.

535   Mekonnen, M. M. and Hoekstra, A. Y.: Water footprint benchmarks for crop production: A first global assessment, Ecol.
Indic., 46, 214–223, https://doi.org/10.1016/j.ecolind.2014.06.013, 2014.

Mialyk, O., Schyns, J. F., Booij, M. J., and Hogeboom, R. J.: Historical simulation of maize water footprints with a new global
gridded crop model ACEA, Hydrol. Earth Syst. Sci. Discuss. [preprint], https://doi.org/10.5194/hess-2021-329 , in review,
2021.

540   Middleton, N. and Thomas, D. S. G.: World atlas of desertification, Arnold, London, UK, 1997.

Moss, R., Babiker, M., Brinkman, S., Calvo, E., Carter, T., Edmonds, J., Elgizouli, I., Emori, S., Erda, L., Hibbard, K., Jones,
R., Kainuma, M., Kelleher, J., Lamarque, J. F., Manning, M., Matthews, B., Meehl, J., Meyer, L., Mitchell, J.,

Nakicenovic, N., O'Neill, B., Pichs, R., Riahi, K., Rose, S., Runci, P., Stouffer, R., van Vuuren, D., Weyant, J., Wilbanks, T., van Ypersele, J. P., and Zurek, M.: Towards New Scenarios for Analysis of Emissions, Climate Change, Impacts, and

545   Response Strategies, IPCC Expert Meeting Report, 19–21 September, 2007, Noordwijkerhout, Netherlands, Intergovernmental Panel on Climate Change (IPCC), Geneva, Switzerland, 132 pp, 2008.

Müller, C., Franke, J., Jägermeyr, J., Ruane, A. C., Elliott, J., Moyer, E., Heinke, J., Falloon, P. D., Folberth, C., Francois, L., Hank, T., César Izaurralde, R., Jacquemin, I., Liu, W., Olin, S., Pugh, T. A. M., Williams, K., and Zabel, F.: Exploring uncertainties in global crop yield projections in a large ensemble of crop models and CMIP5 and CMIP6 climate scenarios,

550   Environ. Res. Lett., 16, 034040, https://doi.org/10.1088/1748-9326/abd8fc, 2021.

Myers, S. S., Smith, M. R., Guth, S., Golden, C. D., Vaitla, B., Mueller, N. D., Dangour, A. D., and Huybers, P.: Climate Change and Global Food Systems: Potential Impacts on Food Security and Undernutrition, Annu. Rev. Public Health, 38, 259–277, https://doi.org/10.1146/annurev-publhealth-031816-044356, 2017.

Navarro-Racines, C., Tarapues, J., Thornton, P., Jarvis, A., and Ramirez-Villegas, J.: High-resolution and bias-corrected

555   CMIP5 projections for climate change impact assessments, Sci. Data, 7, 7, https://doi.org/10.1038/s41597-019-0343-8, 2020.

NBSC: National Data, China, National Bureau of Statistics, Beijing, China, available at: https://data.stats.gov.cn/, 2021.

NOAA: National Oceanic and Atmospheric Administration, U.S, available at: https://www.esrl.noaa.gov, 2018.

O'Neill, B. C., Tebaldi, C., van Vuuren, D. P., Eyring, V., Friedlingstein, P., Hurtt, G., Hurtt, R., Kriegler, E., Lamarque, J.

560   F., Lowe, J., Meehl, G. A., Moss, R., Riahi, K., and Sanderson, B. M.: The Scenario Model Intercomparison Project (ScenarioMIP) for CMIP6, Geosci. Model Dev., 9, 3461–3482, https://doi.org/10.5194/gmd-9-3461-2016, 2016.

Pastor, A. V., Palazzo, A., Havlik, P., Biemans, H., Wada, Y., Obersteiner, M., Kabat, P., and Ludwig, F.: The global nexus of food–trade–water sustaining environmental flows by 2050, Nat. Sustain., 2, 499–507, https://doi.org/10.1038/s41893-019-0287-1, 2019.

565   Portmann, F. T., Siebert, S., and Döll, P.: MIRCA2000-Global monthly irrigated and rainfed crop areas around the year 2000: A new high-resolution data set for agricultural and hydrological modelling, Global Biogeochem. Cy., 24, https://doi.org/10.1029/2008gb003435, 2010.

Qiao, F., Song, Z., Bao, Y., Song, Y., Shu, Q., Huang, C., and Zhao, W.: Development and evaluation of an Earth System Model with surface gravity waves, J. Geophys. Res. Ocean., 118, 4514–4524, https://doi.org/10.1002/jgrc.20327, 2013.

570   Raes, D., Steduto, P., Hsiao, T. C., and Fereres, E.: Reference manual, Chapter 2, AquaCrop model, Version 6.0, Food and Agriculture Organization of the United Nations, Rome, Italy, 2017.

Rallison, R. E.: Origin and evolution of the SCS runoff equation, in: Symposium on Watershed Management, Boise, Idaho, United States, 21–23 July, 912–924, 1980.

Riahi, K., Gruebler, A., and Nakicenovic, N.: Scenarios of long-term socio-economic and environmental development under

575   climate stabilization, Technol. Forecast. Soc. Chang., 74, 887–935, https://doi.org/10.1016/j.techfore.2006.05.026, 2007.

Rosa, L., Chiarelli, D. D., Sangiorgio, M., Beltran-Peña, A. A., Rulli, M. C., D'Odorico, P., and Fung, I.: Potential for sustainable irrigation expansion in a 3 °C warmer climate, Proc. Natl. Acad. Sci. U. S. A., 117, 29526–29534, https://doi.org/10.1073/pnas.2017796117, 2020.

Schmidt, G. A., Kelley, M., Nazarenko, L., Ruedy, R., Russell, G. L., Aleinov, I., Bauer, M., Bauer, S. E., Bhat, M. K., Bleck,
580   R., Canuto, V., Chen, Y. H., Cheng, Y., Clune, T. L., Genio, A. D., Fainchtein, R. D., Faluvegi, G., Hansen, J. E., Healy, R. J., Kiang, N. Y., Koch, D., Lacis, A. A., LeGrande, A. N., Lerner, J., Lo, K. K., Matthews, E. E., Menon, S., Miller, R. L., Oinas, V., Oloso, A. O., Perlwitz, J. P., Puma, M. J., Putman, W. M., Rind, D., Romanou, A., Sato, M., Shindell, D. T., Sun, S., Syed, R. A., Tausnev, N., Tsigaridis, K., Unger, N., Voulgarakis, A., Yao, M. S., and Zhang, J.: Configuration and assessment of the GISS ModelE2 contributions to the CMIP5 archive, J. Adv. Model. Earth Syst., 6,
585   141–184, https://doi.org/10.1002/2013MS000265, 2014.

Schmidt, G. A., Ruedy, R., Hansen, J. E., Aleinov, I., Bell, N., Bauer, M., Bauer, S., Cairns, B., Canuto, V., Cheng, Y., Delgenio, A. D., Faluvegi, G., Friend, A. D., Hall, T. M., Hu, Y., Kelley, M., Kiang, N. Y., Koch, D., Lacis, A. A., Lerner, J., Lo, K. K., Miller, R. L., Nazarenko, L., Oinas, V., Perlwitz, J., Perlwitz, J., Rind, D., Romanou, A., Russell, G. L., Sato, M., Shindell, D. T., Stone, P. H., Sun, S., Tausnev, N., Thresher, D., and Yao, M. S.: Present-Day Atmospheric
590   Simulations Using GISS ModelE: Comparison to In Situ, Satellite, and Reanalysis Data, J. Clim., 19, 153–192, https://doi.org/10.1175/JCLI3612.1, 2006.

Semenov, M. A. and Stratonovitch, P.: Use of multi-model ensembles from global climate models for assessment of climate change impacts, Clim. Res., 41, 1–14, https://doi.org/10.3354/cr00836, 2010.

Tian, Y., Ruth, M., Zhu, D., Ding, J., and Morris, N.: A Sustainability Assessment of Five Major Food Crops' Water Footprints
595   in China from 1978 to 2010, Sustainability, 11, 1–20, https://doi.org/10.3390/su11216179, 2019.

Trnka, M., Feng, S., Semenov, M. A., Olesen, J. E., Kersebaum, K. C., Rötter, R. P., Semerádová, D., Klem, K., Huang, W., Ruiz-Ramos, M., Hlavinka, P., Meitner, J., Balek, J., Havlík, P., and Büntgen, U.: Mitigation efforts will not fully alleviate the increase in water scarcity occurrence probability in wheat-producing areas, Sci. Adv., 5, eaau2406, https://doi.org/10.1126/sciadv.aau2406, 2019.

600   USDA: Estimation of direct runoff from storm rainfall, Section 4 Hydrology, Chapter 4, National Engineering Handbook, Washington DC, USA, 1–24, 1964.

van Vuuren, D. P., den Elzen, M. G. J., Lucas, P. L., Eickhout, B., Strengers, B. J., van Ruijven, B., Wonink, S., and van Houdt, R.: Stabilizing greenhouse gas concentrations at low levels: an assessment of reduction strategies and costs, Clim. Change, 81, 119–159, https://doi.org/10.1007/s10584-006-9172-9, 2007.

605   von Salzen, K., Scinocca, J. F., McFarlane, N. A., Li, J., Cole, J. N. S., Plummer, D., Verseghy, D., Reader, M. C., Ma, X., Lazare, M., and Solheim, L.: The Canadian Fourth Generation Atmospheric Global Climate Model (CanAM4). Part I: Representation of Physical Processes, Atmosphere-Ocean, 51, 104–125, https://doi.org/10.1080/07055900.2012.755610, 2013.

Wang, B., Feng, P., Liu, D. L., O'Leary, G. J., Macadam, I., Waters, C., Asseng, S., Cowie, A., Jiang, T., Xiao, D., Ruan, H.,
He, J., and Yu, Q.: Sources of uncertainty for wheat yield projections under future climate are site-specific, Nat. Food.,
1, 720–728, https://doi.org/10.1038/s43016-020-00181-w, 2020.

Wang, C., Guo, L., Li, Y., and Wang, Z.: Systematic Comparison of C3 and C4 Plants Based on Metabolic Network Analysis,
BMC Syst Biol., 6, S9, https://doi.org/10.1186/1752-0509-6-S2-S9, 2012.

Wang, W., Zhuo, L., Li, M., Liu, Y., and Wu, P.: The Effect of Development in Water-Saving Irrigation Techniques on Spatial-
Temporal Variations in Crop Water Footprint and Benchmarking, J. Hydrol., 577, 123916,
https://doi.org/10.1016/j.jhydrol.2019.123916, 2019.

Xiao, D., Liu, D. L., Wang, B., Feng, P., Bai, H., and Tang, J.: Climate change impact on yields and water use of wheat and
maize in the North China Plain under future climate change scenarios, Agr. Water Manage., 238, 106238, 2020.

Xu, Z., Chen, X., Wu, S. R., Gong, M., Du, Y., Wang, J., Li, Y., and Liu, J.: Spatial-temporal assessment of water footprint,
water scarcity and crop water productivity in a major crop production region, J. Clean. Prod., 224, 375–383,
https://doi.org/10.1016/j.jclepro.2019.03.108, 2019.

Yoon, P. R. and Choi, J. Y.: Efects of shift in growing season due to climate change on rice yield and crop water requirements,
Paddy Water Environ., 18, 291–307, https://doi.org/10.1007/s10333-019-00782-7, 2020.

Zheng, J., Wang, W., Ding, Y., Liu, G., Xing, W., Cao, X., and Chen, D.: Assessment of climate change impact on the water
footprint in rice production: Historical simulation and future projections at two representative rice cropping sites of China,
Sci. Total Environ., 709, 136190, https://doi.org/10.1016/j.scitotenv.2019.136190, 2020.

Zhuo, L., Liu, Y., Yang, H., Hoekstra, A. Y., Liu, W., Cao, X., Wang, M., and Wu, P.: Water for maize for pigs for pork: An
analysis of inter-provincial trade in China, Water Res., 166, 115074, https://doi.org/10.1016/j.watres.2019.115074, 2019.

Zhuo, L., Mekonnen, M. M., and Hoekstra, A. Y.: Benchmark levels for the consumptive water footprint of crop production
for different environmental conditions: a case study for winter wheat in China, Hydrol. Earth Syst. Sci., 20, 4547–4559,
https://doi.org/10.5194/hess-20-4547-2016, 2016a.

Zhuo, L., Mekonnen, M. M., Hoekstra, A. Y., and Wada, Y.: Inter- and intra-annual variation of water footprint of crops and
blue water scarcity in the Yellow River basin (1961–2009), Adv. Water Resour., 87, 29–41,
https://doi.org/10.1016/j.advwatres.2015.11.002, 2016b.

Zhuo, L., Mekonnen, M. M., and Hoekstra, A. Y.: Consumptive water footprint and virtual water trade scenarios for China —
With a focus on crop production, consumption and trade, Environ. Int., 94, 211–223,
https://doi.org/10.1016/j.envint.2016.05.019, 2016c.